Liquid-liquid core-shell configurable mesoscale spherical acoustic lens with subwavelength focusing

Sergio Pérez-López,[1] Pilar Candelas,[1] José Miguel Fuster,[2, a)] Constanza Rubio,[1] Oleg V. Minin,[3, 4] and Igor V. Minin[3, 4]

[1)] *Centro de Tecnologías Físicas, Universitat Politècnica de València, 46022, Spain*

[2)] *Departamento de Comunicaciones, Universitat Politècnica de València, 46022, Spain*

[3)] *Tomsk Polytechnic University, 36 Lenin Avenue, Tomsk 634050, Russia*

[4)] *Tomsk State University, 30 Lenin Avenue, Tomsk 634050, Russia*

In this work, we present a lens based on a thin hollow ABS spherical container structure, which can be filled up with different compatible liquids. The acoustic jet can be dynamically shaped by either shifting the operating frequency or modifying the geometry of the lens. We show for the first time that a spherical Ethanol ABS core-shell acoustical lens immersed in water with low diameter-to-wavelength ratio equal to 6.67 and refractive index of 1.24 achieves a focusing spot narrower than 0.85λ. Experimental measurements validate simulation results and demonstrate the viability of these configurable spherical lenses in underwater acoustic focusing applications.

Wave focusing is a hot topic in several areas of physics, including optics[1,2], microwaves[3,4] and acoustics[5–7]. In this sense, spherical lenses have attracted close attention since the invention of the optical microscope[8]. In acoustics, spherical refractive gas-filled[9] and liquid-filled[10] lenses with high diameter-to-wavelength ratio (D/λ), where the geometrical optics approach is valid, were previously investigated. A liquid-filled acoustic lens with an acoustically transparent spherical shell made of ABS plastic with a relative diameter of $D/\lambda = 17$ at 100 kHz was studied[11]. A liquid-filled spherical acoustic lens with the focal point inside the lens[12] was also investigated. Nevertheless, subwavelength acoustic focusing was never experimentally demonstrated in these works.

Some alternative methods to achieve subwavelength focusing[13,14] include non-linear harmonic generation[15] or time-reversal mirrors[16,17]. However, these alternative methods are low-efficiency processes due to different drawbacks such as ultrasound absorption or low energy translation between frequencies, and thus, spherical lenses are more appealing. Theoretically, based on an analogy to optical photonic nanojet research[18–23], it was recently shown[24,25] that acoustic focusing can be achieved using mesoscale solid or/and metamaterial lenses that produce jet-like focus, known as acoustojets, when the size of the lens is less than 10λ and the geometrical optics approach is not valid. Experimentally, it has been shown that it is possible to obtain a diffraction limited focal spot with mesoscale solid spherical[26] and cylindrical[27] acoustic lenses, which can enhance the capabilities of ultrasound imaging in several areas such as biomedical applications or acoustic microscopy. Acoustic jets are scattered non-evanescent beams of acoustic waves that propagate a short distance through the shadow region of the spherical/cylindrical lens, with subwavelength or even beyond the diffraction limit transversal resolution. The physics behind the jet generation can be described using Mie scattering theory[9,24,26].

It should be noted that there is a fundamental difference in the focusing properties between cylindrical (2D) and spherical (3D) lenses and it is not correct to generalize the results of a 2D lens to a 3D lens directly[28].

Moreover, solid materials with good acoustic properties are extremely rare, and liquid lenses have an advantage over solid lenses because of the lack of transverse sound velocity (shear waves). However, until now, experimental realization of liquid core-shell mesoscale spherical acoustic lens with resolution beyond the wavelength has not been achieved. In this work, we propose a configurable liquid core-shell mesoscale acoustic spherical lens which can modify its acoustic jet-like subwavelength focusing profile.

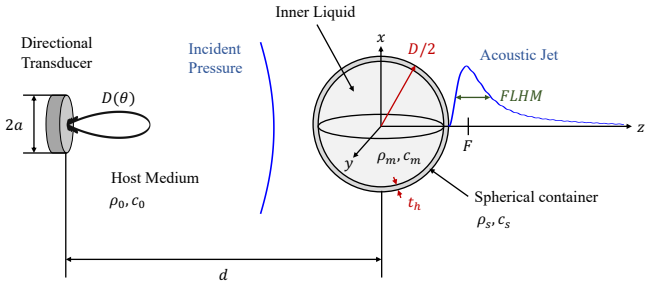

FIG. 1. Schematic of the configurable spherical lens.

Figure 1 depicts a hollow spherical lens of thickness $t_h << \lambda$, where λ is the wavelength in the host medium, and diameter D filled with an inner liquid characterized by its density ρ_m and sound speed c_m. The spherical lens is placed at a distance d from a directional transducer[29] and immersed in a host medium with density ρ_0 and sound speed c_0. The refractive index of the inner liquid is then defined as $n = c_0/c_m$, and provides helpful information about the sound speed contrast between both media. The acoustic jet focusing profile on the near-field region can be shaped by modifying the inner liquid inside the spherical lens, and can be characterized by the focal distance (F), the focal intensity (I_F), the full length half maximum (FLHM) and the full width half maximum (FWHM). These parameters provide information about the jet capability to focus the incident energy into a certain location.

The acoustic pressure generated by the lens has been calculated using a Finite Element Method (FEM) model realized in the commercial software COMSOL Multiphysics. In all sim-

[a)] Electronic mail: jfuster@dcom.upv.es

ulations, the host medium is water and the spherical lens container material is the thermoplastic polymer ABS. The hollow spherical container has a thickness $t_h = 0.25$ mm and an outer diameter $D = 40$ mm. In all simulations, the transducer is modelled as a constant pressure condition of $p_0 = 1$ Pa placed at a distance $d = 350$ mm from the center of the lens.

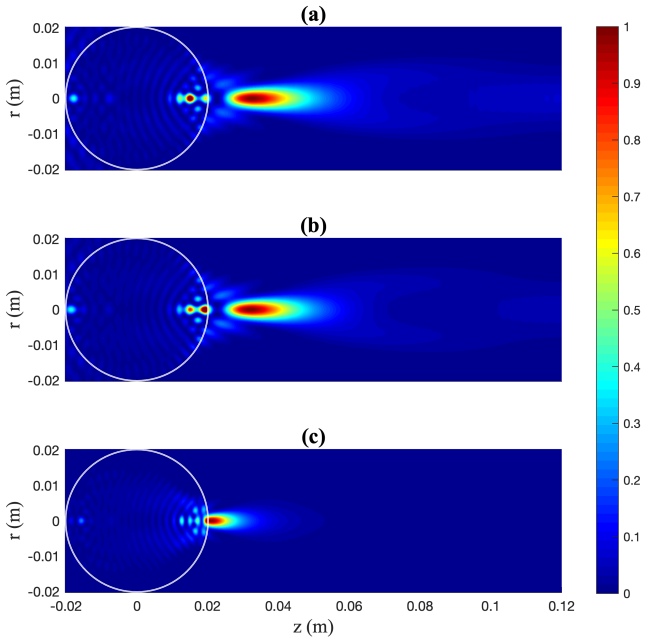

FIG. 2. Normalized intensity maps for different materials: (a) Hexane, (b) Ethanol and (c) Methyl Iodide.

In analogy to optical photonic nanojet research, the surrounding medium should have a lower sound speed than the inner liquid of the lens[24]. Figure 2 shows the numerically computed intensity maps for different inner liquids. Their acoustic properties, as well as those of the host medium and the container material, are shown in Table I for a temperature of $T = 20°$C. In all three cases the operating frequency is set to $f = 250$ kHz, which corresponds to $\lambda = 6$ mm. In this case, $D = 6.67\lambda$ and $t_h = 0.042\lambda$. As it can be observed from Figure 2, the acoustic properties of the inner material have a significant impact on the acoustic jet focusing profile. Figures 2(a), 2(b) and 2(c) show the acoustic jet generated by a hollow spherical lens when the inner liquid is Hexane, Ethanol and Methyl Iodide, respectively. Table II shows the values of all four acoustic jet parameters depicted in Figure 2. Hexane (Figure 2(a)) provides the more extended focal area with the lower focal intensity. Moreover, it corresponds to the wider focal length of 32.5 mm. Ethanol (Figure 2(b)) has a very low refractive index, close to Hexane, and thus it provides a similar focal length of 32 mm. Methyl Iodide (Figure 2(c)) has a higher refractive index than the other two materials, which results in a smaller focal length of 21.05 mm. This material also provides the higher focal intensity and the narrowest lateral resolution (0.472λ) beyond the diffraction limit[19]. To further increase the resolution of this jet, the diameter of the sphere could be augmented. However, Methyl Iodide is a very toxic material and the experimental measurements have been carried out using Ethanol because of Health concerns.

Material	ρ (kg/m^3)	c (m/s)	n
Water	1000	1500	1.00
ABS	1050	2250	0.67
Hexane	655	1203	1.25
Ethanol	789	1207	1.24
Merthyl Iodide	2280	978	1.53

TABLE I. Material acoustic properties.

It is worth noting that despite Hexane having a slightly higher refractive index than Ethanol, it achieves a longer focal distance compared to Ethanol. In optics, a higher refractive index usually results in a shorter focal distance and a higher focal intensity[18,19]. However, mechanical waves behave differently than electromagnetic waves, and as shown in Table I, there are several parameters that influence the focusing properties of the acoustic jet. The difference between the refractive indexes of both Ethanol and Hexane is very low, and both lenses are expected to achieve similar focal distances. Nevertheless, Ethanol has a higher density compared to Hexane, which makes its acoustic impedance higher too. This difference in impedance is the real cause behind the shorter focal distance and the lower intensity level of the Hexane lens compared to the Ethanol lens. Therefore, the density of the inner liquid must also be considered, as it modifies the acoustic impedance of the lens resulting in variations on both focal distance and intensity level.

Material	F (λ)	I_F	FLHM (λ)	FWHM (λ)
Hexane	5.42	0.248	3.085	0.757
Ethanol	5.33	0.339	2.893	0.715
Methyl Iodide	3.51	1.000	–	0.472

TABLE II. Acoustic jet parameters of the different materials shown in Figure 2 ($f = 250$ kHz).

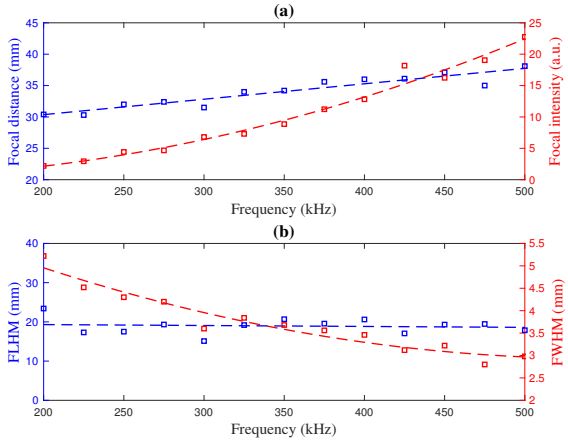

FIG. 3. Acoustic jet parameters as a function of the operating frequency. (a) Focal distance (blue) and focal intensity (red), (b) FLHM (blue) and FWHM (red).

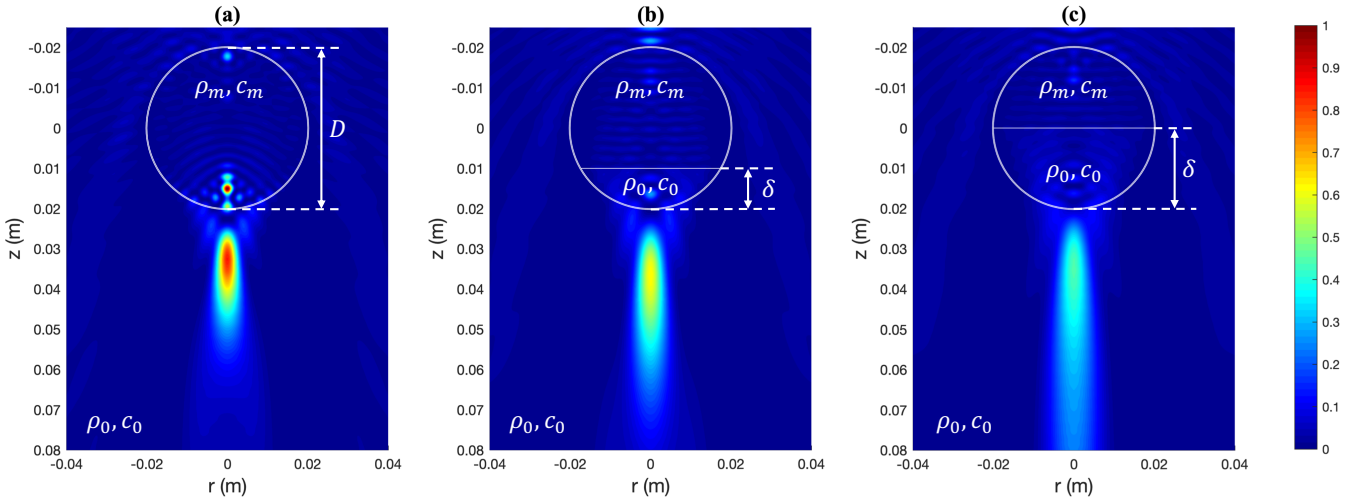

FIG. 4. Simulated intensity maps for different δ values: (a) $\delta = 0$, (b) $\delta = D/4$ and (c) $\delta = D/2$. All values are normalized to the maximum intensity, which in this case is achieved when $\delta = 0$. The frequency is $f = 250$ kHz.

Once the inner liquid has been selected, an interesting parameter which could be used to achieve a finer adjustment onto the focusing profile is the operating frequency. Figure 3 shows the variation of all acoustic jet parameters against the operating frequency when the spherical lens is filled with Ethanol. In the simulations, the incident pressure at the lens is not constant as a directional transducer is being considered. The transducer becomes more directional when frequency is increased, due to its higher size in terms of the wavelength. As it can be observed from Figure 3, the operating frequency induces a linear shift on the focal distance and has almost no effect over the longitudinal resolution, which is determined by the FLHM parameter. The focal intensity increases quadratically with the operating frequency, while the FWHM parameter decreases also with a quadratic tendency, which translates into a higher lateral resolution. Thus, the operating frequency could be used as a dynamic control parameter to linearly shift the focal length.

In order to provide additional control on the acoustic jet focusing profile, the effect of the lens geometry has also been considered[30–32]. When the lens inner liquid is immiscible with the host medium, the geometry of the acoustic lens can be dynamically modified by introducing a certain amount of the host medium liquid inside the lens. Neglecting the thickness of the sphere, the resulting structure behaves as a truncated spherical lens, where the size of the truncated section depends on the amount of host medium introduced inside the lens. The variation on the lens geometry can be implemented by attaching an input and output connection to the lens container. The input connection allows the introduction of the desired amount of host medium liquid, while the exceeding inner liquid is evacuated through the output connection. This mechanism provides a dynamical and fast procedure to modify the focusing profile of the acoustic jet.

Figure 4 shows simulation results for three configurations in which different amounts of host medium liquid have been introduced inside the lens. The host medium is water and the inner liquid is Hexane, an hydrocarbon immiscible with water. As water is denser than Hexane, it occupies the bottom of the spherical lens, while Hexane is isolated on top of the water layer. The directional transducer is located in this case above the lens pointing downwards and the acoustic jet is oriented vertically as shown in Figure 4. A design parameter, δ, depicted in Figures 4(b) and 4(c), has been defined as the axial length corresponding to the volume of host medium liquid inside the lens. As it can be observed from Figure 4, when the spherical lens is truncated, the focal area is outspread, decreasing the focal intensity while both the FWHM and the FLHM parameters increase their values.

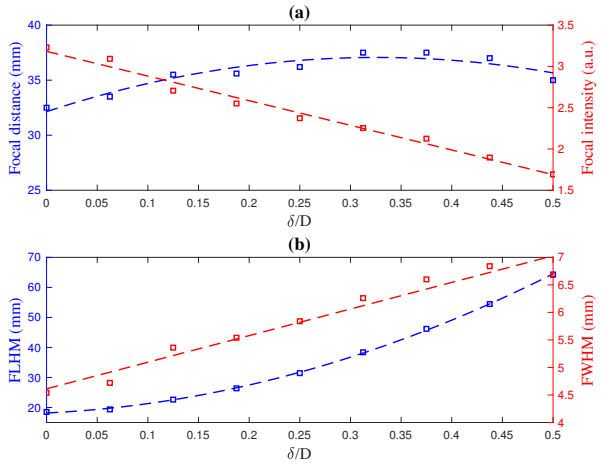

FIG. 5. Acoustic jet parameters as a function of δ. (a) Focal distance (blue) and focal intensity (red), (b) FLHM (blue) and FWHM (red). $f = 250$ kHz.

Figure 5 shows the variation of all acoustic jet parameters against δ when the inner liquid is Hexane and the host medium is water. The focal length varies quadratically with δ

with a local maximum around $\delta = 0.3$. Besides, when the δ parameter augments its value, that is when the truncated size becomes larger, both FLHM and FWHM parameters increase while the focal intensity diminishes almost linearly. Therefore, the variation of the lens geometry can be used to dynamically soften and spread out the focal area of the acoustic jet.

An alternative control parameter would be the volume fraction, V_F, that is the ratio between the host medium volume inside the lens and the total liquid volume (host medium and inner liquid). The V_F parameter can be easily computed and is related to the δ/D parameter through the following expression

$$V_F = \frac{V_{hm}}{V_{total}} = 3\left(\frac{\delta}{D}\right)^2 - 2\left(\frac{\delta}{D}\right)^3, \qquad (1)$$

with $V_{total} = V_{il} + V_{hm}$, being V_{il} the inner liquid volume and V_{hm} the host medium volume inside the lens.

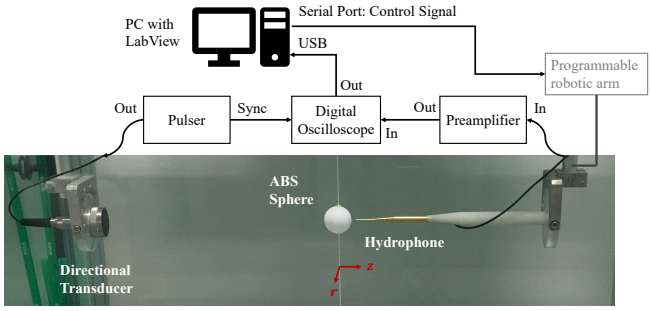

FIG. 6. Experimental Set-up.

Experimental measurements have been carried out in order to validate the configurable spherical lens. Figure 6 shows the experimental set-up, where an underwater 3D automated positioning system with a spatial resolution of $1 \times 1 \times 1$ mm^3 is used inside a water tank. An Imasonic 250 kHz piston transducer with a 30 mm active diameter is used as emitter. A needle hydrophone from Precision Acoustics Ltd., with a diameter of 1.5 mm, is used as receiver. The transmitted signal is generated using a Panametrics 5077PR Pulser, whereas the received signal is acquired and sampled using a digital oscilloscope from Pico Technology. The measurement process is automated using a LabView program, which controls both the robotic arm and the digital oscilloscope.

Figures 7(a) and 7(b) show simulated and measured intensity maps, respectively, for a frequency of $f = 250$ kHz. Figures 8(a) and 8(b) depict the longitudinal and radial cuts of the intensity maps shown in Figure 7. Simulations are depicted in red, while the blue lines correspond to experimental measurements. As it can be observed from Figures 7 and 8, simulations and experimental measurements agree very well, validating the use of these configurable spherical lenses for underwater ultrasound focusing. As it can be observed from Figure 8(a), the measured focal distance ($F = 32.00$ mm) is identical to that simulated with the FEM software. However, the focal area spreads out slightly in the experimental measurements in comparison to the simulation results. Thus, the

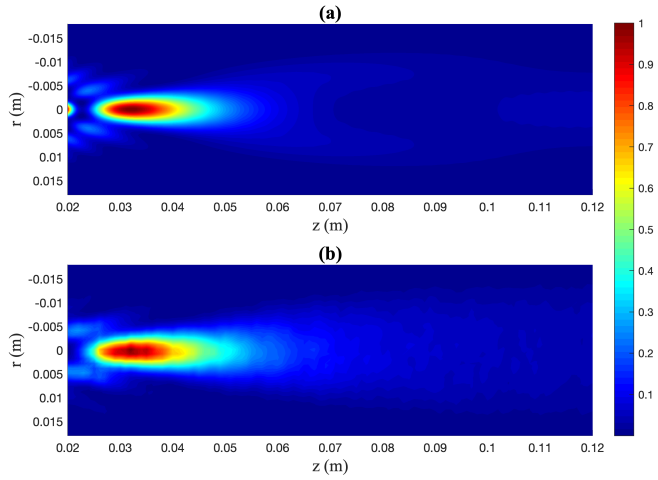

FIG. 7. Normalized intensity maps: (a) simulation results and (b) experimental measurements.

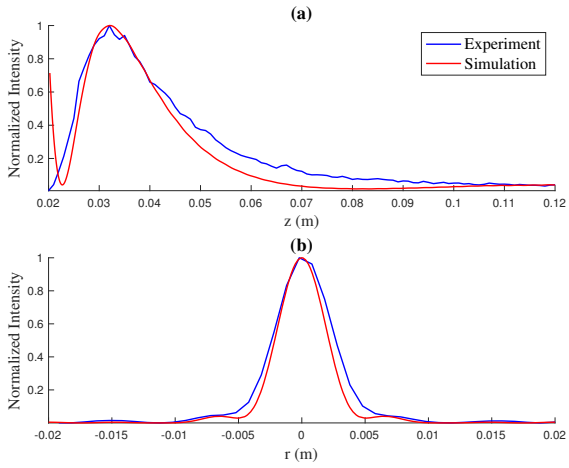

FIG. 8. (a) Longitudinal cut ($r = 0$) and (b) transversal cut ($z = F$). Experimental measurements (blue lines) and simulation results (red lines).

measured FLHM and FWHM are 3.330λ and 0.847λ, respectively, which result in an increase of 13.07% and 18.69% compared to their simulated counterparts.

In this paper, a configurable liquid-liquid core-shell mesoscale spherical acoustic lens with a diameter of 6.67λ and a refractive index of 1.24 capable of providing subwavelength resolution has been proposed. The choice of the inner liquid allows a coarse control of the acoustic jet properties. Once the inner liquid is selected, finer tunability can be achieved by shifting the operating frequency, which has a significant effect over the focal intensity and the FWHM parameter. Moreover, if the inner liquid is immiscible with the host medium, additional control on the jet focusing profile can be provided by introducing a certain amount of the host medium liquid inside the hollow sphere and thus, modifying the geometry of the lens. An Ethanol-filled lens with an ABS shell has

been experimentally characterized, showing good agreement with numerical simulations and providing a simple method to achieve subwavelength focusing (0.847λ). It has also been shown that the use of an inner liquid with a lower sound speed leads to an increase in lateral resolution beyond the diffraction limit. Thus, this work opens new possibilities to implement and design compact focusing/imaging systems with high resolution and controllable focal distances, that can be appealing to numerous researchers working in the acoustics field.

ACKNOWLEDGMENTS

This work has been supported by Spanish MINECO TEC2015-70939-R and MICINN RTI2018-100792-B-I00 projects. S.P.-L. acknowledges financial support from Universitat Politècnica de València grant program PAID-01-18. I.V.M. and O.V.M. acknowledge the Tomsk Polytechnic University Competitiveness Enhancement Program.

[1] Q. Meng, X. Zhang, L. Cheng, P. Cao, Y. Li, H. Zhang, and G. Wang, "Deep subwavelength focusing of light by a trumpet hyperlens," Journal of Optics **13**, 075102 (2011).

[2] M. Papaioannou, E. Plum, E. T. Rogers, and N. I. Zheludev, "All-optical dynamic focusing of light via coherent absorption in a plasmonic metasurface," Light: Science & Applications **7**, 17157–17157 (2018).

[3] H. D. Hristov and J. M. Rodriguez, "Design Equation for Multidielectric Fresnel Zone Plate Lens," IEEE Microwave and Wireless Components Letters **22**, 574–576 (2012).

[4] T. Ding, J. Yi, H. Li, H. Zhang, and S. N. Burokur, "3D field-shaping lens using all-dielectric gradient refractive index materials," Scientific Reports **7**, 782 (2017).

[5] N. Jiménez, V. Romero-García, R. Picó, L. M. Garcia-Raffi, and K. Staliunas, "Nonlinear focusing of ultrasonic waves by an axisymmetric diffraction grating embedded in water," Applied Physics Letters **107**, 204103 (2015).

[6] Y. Ge, H.-x. Sun, C. Liu, J. Qian, S.-q. Yuan, J.-p. Xia, Y.-j. Guan, and S.-y. Zhang, "Acoustic focusing by an array of heat sources in air," Applied Physics Express **9**, 066701 (2016).

[7] J.-p. Xia, H.-x. Sun, Q. Cheng, Z. Xu, H. Chen, S.-q. Yuan, S.-y. Zhang, Y. Ge, and Y.-j. Guan, "Theoretical and experimental verification of acoustic focusing in metal cylinder structure," Applied Physics Express **9**, 057301 (2016).

[8] R. Hooke, *Micrographia, or some Physiological Descriptions of Minute Bodies, made by Magnifying Glasses, with Observations and Inquiries thereupon* (printed by J. Martyn and J. Allestry, Royal Society, London, 1665).

[9] D. C. Thomas, K. L. Gee, and R. S. Turley, "A balloon lens: Acoustic scattering from a penetrable sphere," American Journal of Physics **77**, 197–203 (2009).

[10] G. C. Knollman, J. L. S. Bellin, and J. L. Weaver, "Variable-Focus Liquid-Filled Hydroacoustic Lens," The Journal of the Acoustical Society of America **49**, 253–261 (1971).

[11] E. Belcher, "A multibeam, diver-held sonar using a liquid-filled, spherical acoustic lens," in *Proceedings of OCEANS '93* (IEEE, 2002) pp. III398–III402.

[12] S. M. Hasheminejad and M. Azarpeyvand, "Sound radiation from a liquid-filled underwater spherical acoustic lens with an internal eccentric baffled spherical piston," Ocean Engineering **31**, 1129–1146 (2004).

[13] T. Liu, F. Chen, S. Liang, H. Gao, and J. Zhu, "Subwavelength Sound Focusing and Imaging Via Gradient Metasurface-Enabled Spoof Surface Acoustic Wave Modulation," Physical Review Applied **11**, 034061 (2019).

[14] F. Ma, J. Chen, and J. H. Wu, "Three-dimensional acoustic sub-diffraction focusing by coiled metamaterials with strong absorption," Journal of Materials Chemistry C **7**, 5131–5138 (2019).

[15] D. Rugar, "Resolution beyond the diffraction limit in the acoustic microscope: A nonlinear effect," Journal of Applied Physics **56**, 1338–1346 (1984).

[16] J. de Rosny and M. Fink, "Overcoming the Diffraction Limit in Wave Physics Using a Time-Reversal Mirror and a Novel Acoustic Sink," Physical Review Letters **89**, 124301 (2002).

[17] A. Sarvazyan, L. Fillinger, and L. R. Gavrilov, "Time-reversal acoustic focusing system as a virtual random phased array," IEEE Transactions on Ultrasonics, Ferroelectrics and Frequency Control **57**, 812–817 (2010).

[18] A. Heifetz, S.-C. Kong, A. V. Sahakian, A. Taflove, and V. Backman, "Photonic Nanojets," Journal of Computational and Theoretical Nanoscience **6**, 1979–1992 (2009).

[19] B. S. Luk'yanchuk, R. Paniagua-Domínguez, I. Minin, O. Minin, and Z. Wang, "Refractive index less than two: photonic nanojets yesterday, today and tomorrow [Invited]," Optical Materials Express **7**, 1820 (2017).

[20] P. Wu, J. Li, K. Wei, and W. Yue, "Tunable and ultra-elongated photonic nanojet generated by a liquid-immersed core–shell dielectric microsphere," Applied Physics Express **8**, 112001 (2015).

[21] L. Yue, B. Yan, J. N. Monks, Z. Wang, N. T. Tung, V. D. Lam, O. Minin, and I. Minin, "Production of photonic nanojets by using pupil-masked 3D dielectric cuboid," Journal of Physics D: Applied Physics **50**, 175102 (2017).

[22] L. Yue, B. Yan, J. N. Monks, R. Dhama, Z. Wang, O. V. Minin, and I. V. Minin, "Intensity-Enhanced Apodization Effect on an Axially Illuminated Circular-Column Particle-Lens," Annalen der Physik **530**, 1700384 (2018).

[23] L. Yue, O. V. Minin, Z. Wang, J. N. Monks, A. S. Shalin, and I. V. Minin, "Photonic hook: a new curved light beam," Optics Letters **43**, 771 (2018).

[24] O. V. Minin and I. V. Minin, "Acoustojet: acoustic analogue of photonic jet phenomenon based on penetrable 3D particle," Optical and Quantum Electronics **49**, 54 (2017).

[25] J. H. Lopes, J. P. Leão-Neto, I. V. Minin, O. V. Minin, and G. T. Silva, "A theoretical analysis of jets," in *22nd International Congress on Acoustics* (Buenos Aires, Argentina, 2016).

[26] J. H. Lopes, M. A. B. Andrade, J. P. Leão-Neto, J. C. Adamowski, I. V. Minin, and G. T. Silva, "Focusing Acoustic Beams with a Ball-Shaped Lens beyond the Diffraction Limit," Physical Review Applied **8**, 024013 (2017).

[27] I. Minin and O. Minin, "Mesoscale Acoustical Cylindrical Superlens," MATEC Web of Conferences **155**, 01029 (2018).

[28] Y. E. Geints, A. A. Zemlyanov, O. V. Minin, and I. V. Minin, "Systematic study and comparison of photonic nanojets produced by dielectric microparticles in 2D- and 3D-spatial configurations," Journal of Optics **20**, 065606 (2018).

[29] S. Pérez-López, J. M. Fuster, P. Candelas, C. Rubio, and F. Belmar, "On the use of phase correction rings on Fresnel zone plates with ultrasound piston emitters," Applied Physics Letters **112**, 264102 (2018).

[30] C.-Y. Liu, "Photonic nanojet shaping of dielectric non-spherical microparticles," Physica E: Low-dimensional Systems and Nanostructures **64**, 23–28 (2014).

[31] D. Li, X. Wang, J. Ling, and H. Yuan, "Super-narrow focusing and ultra-long working distance by different shapes of dielectric microlenses," Optik **160**, 138–145 (2018).

[32] Y. Zhou, Y. Tang, Y. He, X. Liu, and S. Hu, "Effects of immersion depth on super-resolution properties of index-different microsphere-assisted nanoimaging," Applied Physics Express **11**, 032501 (2018).